Gondwana Research 87 (2020) 248–262

Contents lists available at ScienceDirect

Gondwana Research

journal homepage: www.elsevier.com/locate/gr

Paleo- to Mesoproterozoic magmatic and tectonic evolution of the southwestern Yangtze Block, south China: New constraints from ca. 1.7–1.5 Ga mafic rocks in the Huili-Dongchuan area

Hong-Peng Fan [a], Wei-Guang Zhu [a,*], Zheng-Xiang Li [b]

[a] State Key Laboratory of Ore Deposit Geochemistry, Institute of Geochemistry, Chinese Academy of Sciences, 99 West Lincheng Road, Guiyang 550081, China
[b] ARC Center of Excellence for Core to Crust Fluid Systems (CCFS) and The Institute for Geoscience Research (TIGeR), Department of Applied Geology, Curtin University, GPO Box U1987, Perth, Western Australia 6845, Australia

ARTICLE INFO

Article history:
Received 7 December 2019
Received in revised form 11 June 2020
Accepted 26 June 2020
Available online 20 August 2020

Handling Editor: Y.P. Dong

Keywords:
Mantle plume
Paleo- to Mesoproterozoic
Mafic magmatism
Tong'an Group
Yangtze Block

ABSTRACT

Paleo- to early Mesoproterozoic rocks in the Yangtze Block are extremely sparse and are predominately exposed along the southwestern margin. Their petrogenesis and tectonic significance remain unclear, resulting in a limited understanding of the tectonic evolution of the southwestern Yangtze Block during this period. Therefore, we report here detailed geochronological and geochemical analyses of newly discovered Paleo- to early Mesoproterozoic mafic intrusive rocks in the Huili-Dongchuan area, southwestern Yangtze Block and interpret their petrogenesis and tectonic significance. Secondary ion mass spectroscopy (SIMS) zircon and baddeleyite U-Pb dating yielded crystallization ages of ca. 1716–1714 Ma for gabbros and diabases (referred to as the 1.72–1.71 Ga group), ca. 1705–1700 Ma for gabbros and a diabase-porphyrite (the 1.70 Ga group), and ca. 1519–1504 Ma for a gabbro and a diabase (the 1.52–1.50 Ga group), which effectively constrain the minimum depositional age of the Tong'an and Dongchuan groups that they intrude to 1.72 Ga. The three groups (or episodes) of intrusive rocks differ from each other in their chemical compositions and isotopic characteristics, most likely because of varying degrees of melting in a convective upper mantle (probably the asthenosphere), which had been metasomatized by melts with enriched components input by a plume from the lower mantle. Modeling calculations suggest that fractional crystallization (FC) and assimilation and fractional crystallization (AFC) were the most important processes involved in modifying the chemical compositions of these rocks. These magmatic activities are interpreted to have been related to mantle plumes and continental rifting that occurred in the Huili-Dongchuan area near the southwestern margin of the Yangtze Block.

1. Introduction

The Yangtze Block is one of the largest ancient continental crust blocks in eastern Asia. Recent studies highlight Archean basement evolution of the Yangtze Block (e.g., Li et al., 2014; Hui et al., 2017; Wang et al., 2018; and references therein). The subsequent Paleo- to Mesoproterozoic history of the Yangtze Block has attracted increasing research attention because of its possible involvement in the assembly and breakup of the Paleo- to Mesoproterozoic supercontinent Nuna (also known as Columbia; e.g., Rogers and Santosh, 2002; Zhao et al., 2002; Ernst et al., 2008; Evans and Mitchell, 2011; Meert, 2012; Wang et al., 2012; Fan et al., 2013; Chen et al., 2013; Wang and Zhou, 2014; Zhou et al., 2014; Meert and Santosh, 2017; Lu et al., 2019; Cui et al., 2019) as well as the presence of large Fe–Cu–rare earth element (REE) deposits (e.g., the Dahongshan, Lala, Yinachang, Xikuangshan and Sin Quyen deposits; Zhou et al., 2014; and references therein) and Fe-Ti-V oxide ore deposits (such as the Zhuqing deposit; Fan et al., 2013, 2014) in the late Paleoproterozoic to early Mesoproterozoic rocks of the southwestern part of the block.

Nevertheless, outcrops of Paleo- to Mesoproterozoic rock units (e.g. the Tianli schists and the Dahongshan, Hekou, Dongchuan and Tong'an groups) (e.g., Greentree et al., 2006; Li et al., 2007, 2014; Greentree and Li, 2008; Zhao et al., 2010; Peng et al., 2012; Fan et al., 2013; Zhou et al., 2014) and 1.7–1.5 Ga intrusive and metavolcanic rocks (e.g., Zhao et al., 2010; Fan et al., 2013; Chen et al., 2013; Lu et al., 2019; Zhu et al., 2016a, 2017, 2019) are extremely sparse, and have been identified mostly in the Kangdian region of southwestern Yangtze Block (Fig. 1). As a consequence, the stratigraphy of these Paleo- to Mesoproterozoic rock units has been long debated due to few constraints on the ages of them (e.g., Zhao et al., 2010; Fan et al., 2013; Zhou et al., 2014). Moreover, the lack of systematic geochronological, geochemical, and isotope

* Corresponding author.
E-mail address: zhuweiguang@vip.gyig.ac.cn (W.-G. Zhu).

https://doi.org/10.1016/j.gr.2020.06.019
1342-937X/

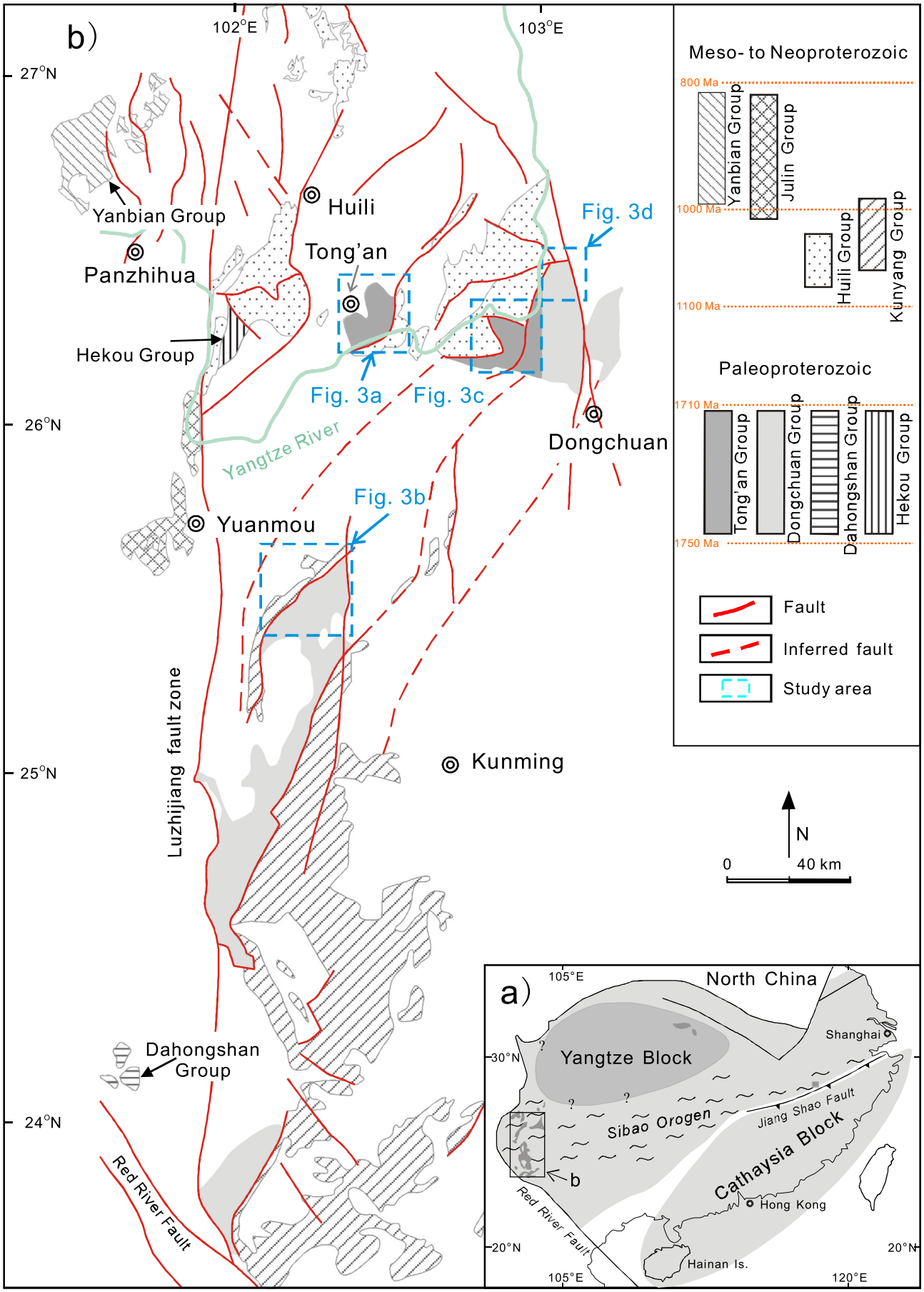

Fig. 1. a) Simplified tectonic map showing the study area in relation to South China's major tectonic units (Li et al., 2007); b) geological map of the late Paleo- to Mesoproterozoic strata and Proterozoic intrusions in the Kangdian region, SW China (modified after Wu et al., 1990).

studies of the intrusive and metavolcanic rocks has prevented a comprehensive understanding of the Paleo- to Mesoproterozoic evolution of the Yangtze Block.

In this contribution, we report the results of a detailed study of several recently discovered mafic intrusions that intrude the Paleoproterozoic Dongchuan and Tong'an groups in the Huili–Dongchuan area (Fig. 1). On the basis of precise ages and distinguishable geochemical compositions, the studied mafic rocks can be subdivided into three groups: a 1.72–1.71 Ga group of gabbros and diabases with ages of 1716–1714 Ma, a 1.70 Ga group of gabbros and a diabase-porphyrite with ages of 1705–1700 Ma, and a 1.52–1.50 Ga group of a gabbro and a diabase with ages of 1519–1504 Ma. Taking into account preciously reported geochemical and isotopic data for some of these intrusions (Fan et al., 2013; Chen et al., 2013; Zhu et al., 2016a, 2017, 2019; Lu et al., 2019), we use our new data to assess the origin of these rocks and to discuss the implications for regional stratigraphic correlation and tectonic evolution of the southwestern Yangtze Block during the late Paleo- to Mesoproterozoic.

2. Geological background and petrography

2.1. Regional geology

The Yangtze Block and the Cathaysia Block was joined by the late-Mesoproterozoic to earliest Neoproterozoic Sibao Orogen to form the South China Block (Li et al., 2007) (Fig. 1a). In the Yangtze Block, Archaean–Palaeoproterozoic basement rocks crop out mainly in the northern part, whereas late Palaeoproterozoic basement rocks are found in the southwestern part of the block, known as the Kangdian region (Fig. 1b). The oldest supracrustal in this area are the late Paleoproterozoic Dahongshan, Hekou, Dongchuan, and Tong'an groups. The Meso- to Neoproterozoic Huili, Kunyang, Yanbian and Julin groups occur along the Luzhijiang fault and related NNE-trending faults (Wu et al., 1990; Greentree and Li, 2008; Zhao et al., 2010; Fan et al., 2013) (Figs. 1b and 2).

The Dahongshan, Hekou, Dongchuan, and Tong'an groups host mafic intrusions and meta-volcanic layers with zircon U-Pb ages of 1.7–1.5 Ga (Greentree and Li, 2008; He, 2009; Zhao et al., 2010; Zhao and Zhou, 2011; Fan et al., 2013; Chen et al., 2013; Zhu et al., 2016a, 2017), and these groups have been suggested to be lateral equivalents (Fan et al., 2013). Nevertheless, the Dahongshan and Hekou groups consist of metavolcanic and metasedimentary rocks that were metamorphosed under conditions of upper greenschist to lower amphibolite facies metamorphism, whereas the Dongchuan and Tong'an groups underwent lower greenschist facies metamorphism (Wu et al., 1990).

The Huili and Kunyang groups consist of thick sequences of siliciclastic, volcanic, and carbonate rocks with ~1.0 Ga meta-volcanic layers (Greentree et al., 2006; Zhang et al., 2007; Zhu et al., 2016b). The Yanbian Group of earliest Neoproterozoic age consists of strongly deformed and variably metamorphosed clastic rocks and pillow lavas basalts (Sun et al., 2009; Li et al., 2006). The Julin Group has been locally metamorphosed to lower amphibolite facies, and the metabasalts have ages of ca. 1050 Ma (Chen et al., 2014). These rocks are overlain by a thick sequence (maximum >9 km) of Neoproterozoic (850–540 Ma) to Permian strata comprising clastic, carbonate and volcanic rocks.

2.2. The Tong'an and Dongchuan groups and associate mafic rocks

The Precambrian units in the Kangdian region have poor age constraints because of the sparse outcrops and the fact that the stratigraphic units in this region are often in fault contact with each other owing to the strongly regional fault development (Wu et al., 1990).

The traditional Tong'an Formation is made up of Yinmin (TA1), Luoxue (TA2), Heishan (TA1), Qinglongshan (TA4) and Tangtang (TA5) sub-formations, which was included as a part of the Huili Group by early regional mapping (SBG, 1967) (Fig. 2a). This stratigraphic scheme was subsequently refined as a result of more detailed mapping

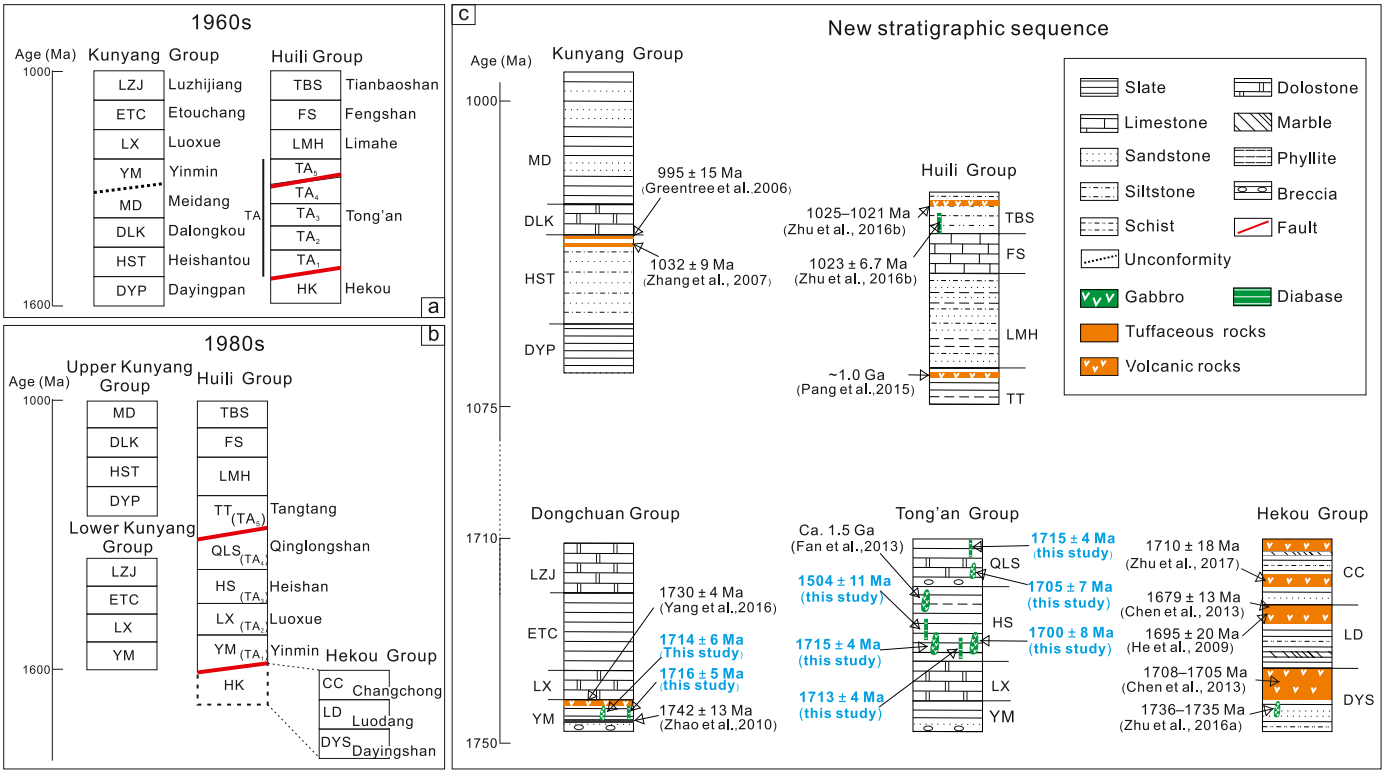

Fig. 2. Simplified stratigraphic correlations for the Paleo- to Mesoproterozoic Hekou, Tong'an, Dongchuan, Huili and Kunyang groups in the Kangdian region, western Yangtze Block, SW China.

work (Wu et al., 1990) (Fig. 2b). However, newly reported isotope ages and fieldwork show that the lower parts of the traditional Huili and Kunyang groups are comparable but are separated from their upper parts by a depositional hiatus (Fig. 2c) (e.g., Li et al., 1988; Wu et al., 1990; Geng et al., 2007; Zhao et al., 2010; Fan et al., 2013; Chen et al., 2013; Zhou et al., 2014; Pang et al., 2015; Yang et al., 2016; Gao et al., 2018). Therefore, in this study, we include the lower parts of the traditional Huili Group (the Yinmin, Luoxue, Heishan and Qinglongshan formations) as the Tong'an Group and refer the upper parts of the traditional Huili Group (the Tangtang, Limahe, Fengshan and Tianbaoshan formations) as the Huili Group (Fig. 2c).

The Tong'an Group consists of, from the base upward, the Yinmin, Luoxue, Heishan, and Qinglongshan formations which are commonly in fault contact with each other and have been tightly foliated and

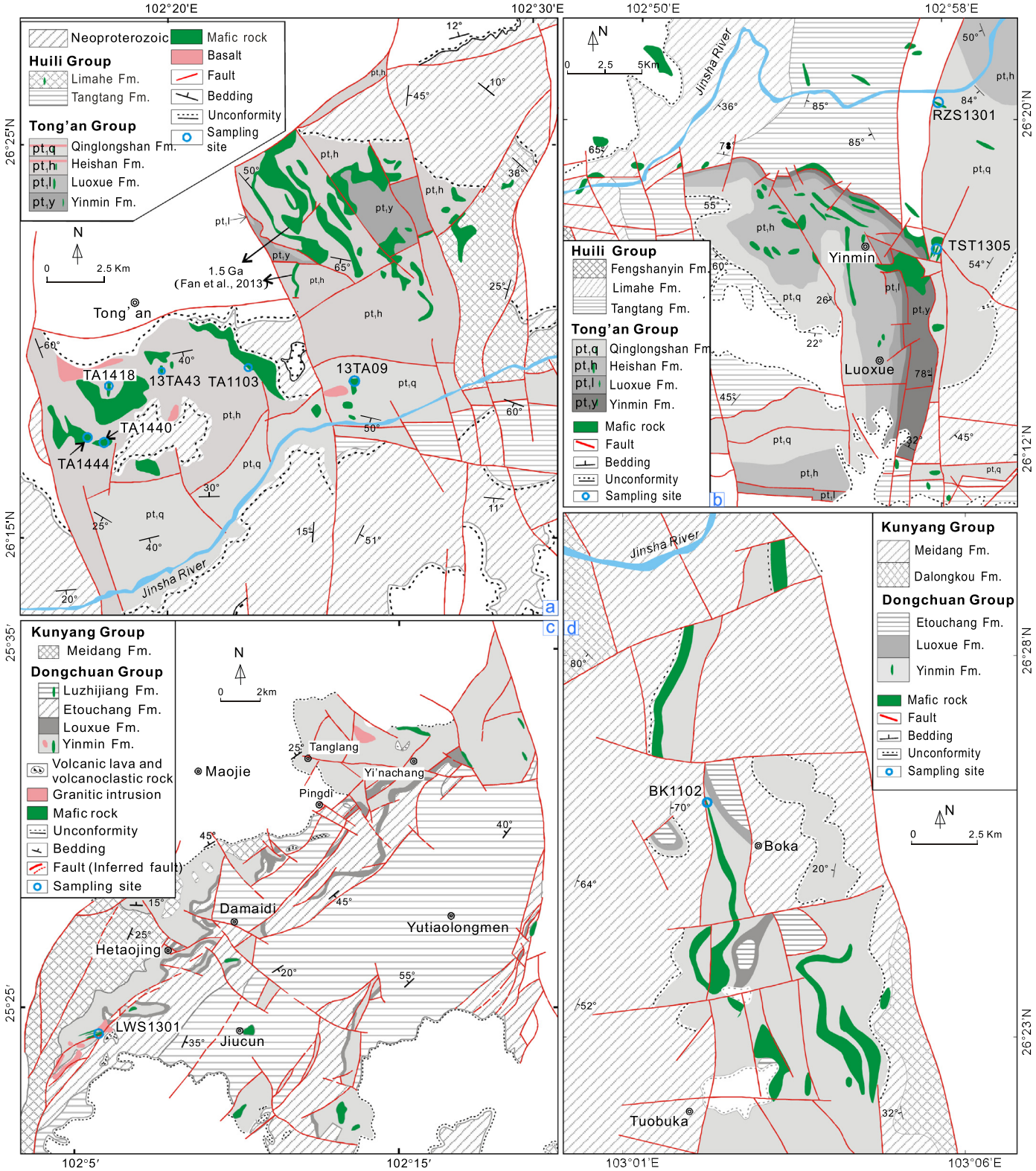

Fig. 3. Simplified geological map showing the Paleo- to earliest Neoproterozoic rocks in the a) Tong'an, b) Yinmin, c) Yi'nachang and d) Boka regions and sampling locations.

folded (Fig. 2c). The Dongchuan Group comprises the Yinmin, Luoxue, Etouchang, and Luzhijiang formations from the base upward (Fig. 2c). The Dongchuan sediments contain detrital zircons with a youngest age population of ~1.78 Ga, and layers of tuff and rhyolite have yielded zircon U-Pb ages of 1742 ± 13 Ma (Zhao et al., 2010) and 1730 ± 4 Ma (Yang et al., 2016), respectively. These two groups were intruded by a number of irregular plugs and dikes of either alkaline or tholeiitic basaltic rocks, and less commonly by felsic rocks (Fig. 3a–d), none of which have been well studied. These plutons are commonly sill-like, measure up to 10 km in length and mostly 90–300 m in width, strike roughly NW–SE, and dip to the SW (Fig. 3). They show variable degrees of alteration and contain anhedral crystals of plagioclase, clinopyroxene, Fe-Ti oxides (magnetite and ilmenite), and minor amounts of hornblende, biotite, apatite, and sulfide minerals (pyrite and chalcopyrite) (Fig. 4). The exact shapes of the mafic intrusions are hard to identify due to well-developed cleavages in both the intruded and wall rocks (Figs. 3 and 4).

3. Sampling and analytical methods

More than one hundred and fifty samples were collected from the best-exposed and least-altered outcrops of four diabase dikes, six gabbroic plutons and a diabase-porphyrite pluton in the Huili–Dongchuan area (Figs. 2c and 3). Thin sections were prepared for all samples and seventy-nine least altered samples were chosen for whole rock analysis, among which, ten representative samples were selected for zircon and baddeleyite U-Pb dating, and thirty-two samples were used for Nd isotopic analysis.

Zircon grains from samples TST1305, BK1102, TA1444, TA1440, TA1309 and 13TA09, and baddeleyite grains from samples TST1305, LWS1301, TA1103, TA1418 and RZS1301 were obtained using conventional heavy liquid and magnetic techniques. Hand-picked zircon and baddeleyite grains were then mounted in epoxy resin discs. To identify grains for dating, the grains were documented with transmitted and reflected light micrographs as well as cathodoluminescence (CL) after having been polished. Finally, they were coated with gold to be prepared for analyze. U-Pb dating were conducted using a Cameca IMS 1280 ion microprobe (SIMS) at the Institute of Geology and Geophysics, the Chinese Academy of Sciences (CAS) in Beijing. Detailed analytical procedures for zircon and baddeleyite U-Pb dating can be found in Li et al. (2009) and Li et al. (2010), respectively. The SIMS U-Pb zircon and baddeleyite ages are presented in Supplementary Table S1.

Whole-rock major element compositions were determined using X-ray fluorescence spectrometers (XRF) at ALS Chemex Co Ltd.,

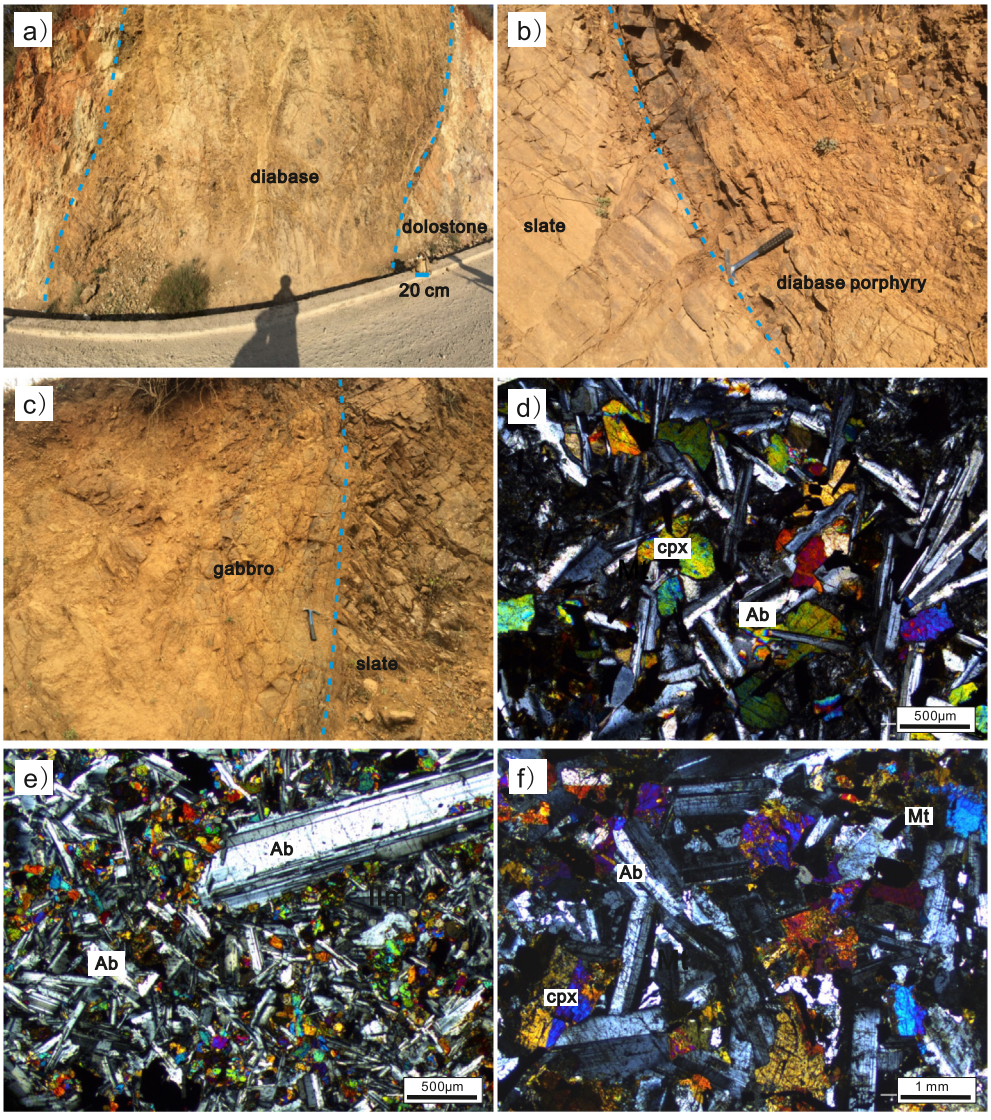

Fig. 4. Representative field photos and microscopic photographs of a) and d) a diabase dike, b) and e) a diabase-porphyrite pluton, and c) and f) a gabbroic pluton from the Huili–Dongchuan area, respectively. Cpx = clinopyroxene, Ab = albite, Mt. = magnetite.

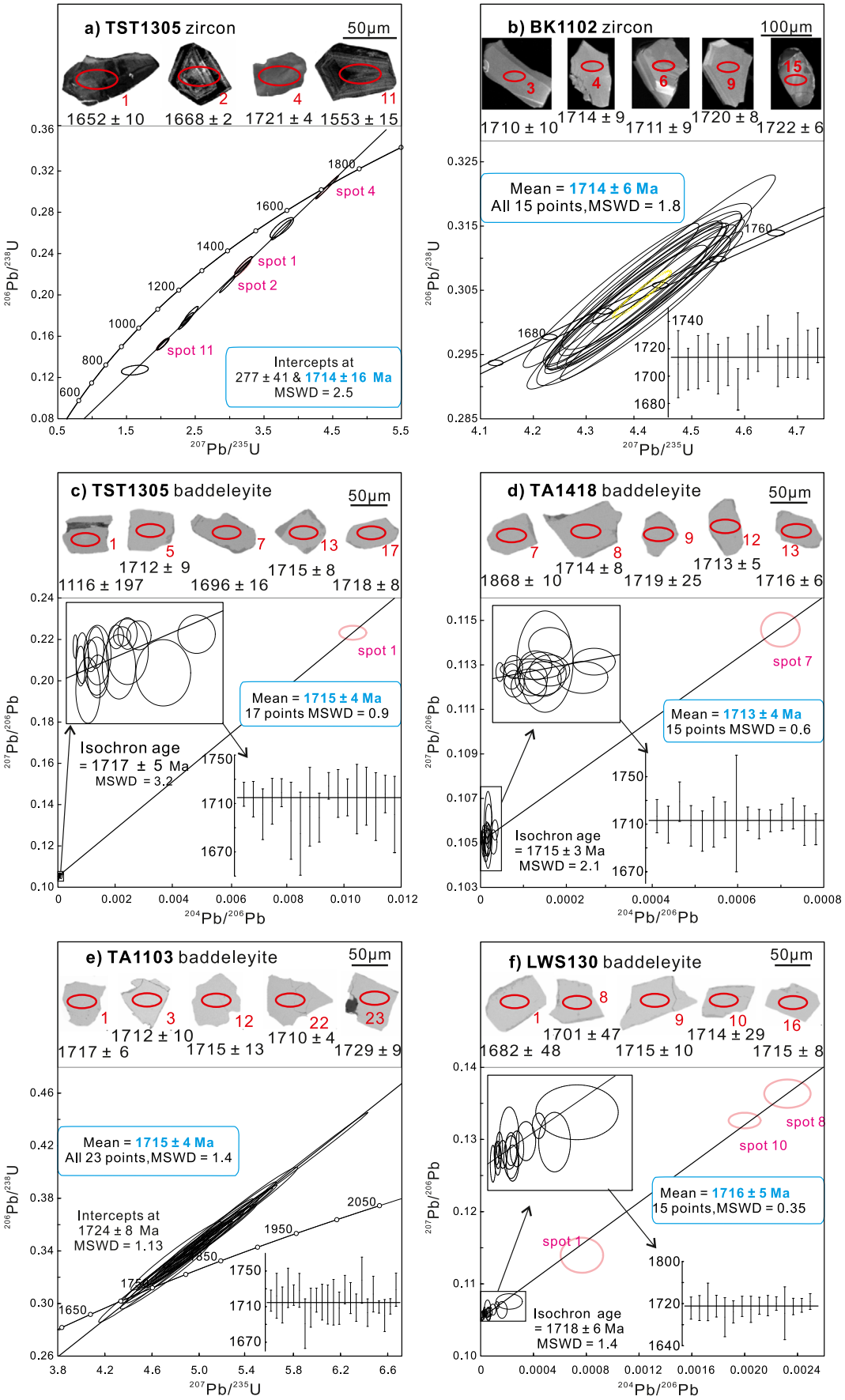
a) TST1305 zircon
50μm
1
2
4
11
1652 ± 10
1668 ± 2
1721 ± 4
1553 ± 15
spot 4
spot 1
spot 2
spot 11
Intercepts at
277 ± 41 & 1714 ± 16 Ma
MSWD = 2.5
b) BK1102 zircon
100μm
3
4
6
9
15
1710 ± 10
1714 ± 9
1711 ± 9
1720 ± 8
1722 ± 6
Mean = 1714 ± 6 Ma
All 15 points,MSWD = 1.8
c) TST1305 baddeleyite
50μm
1
5
7
13
17
1712 ± 9
1116 ± 197
1696 ± 16
1715 ± 8
1718 ± 8
spot 1
Mean = 1715 ± 4 Ma
17 points MSWD = 0.9
Isochron age
= 1717 ± 5 Ma
MSWD = 3.2
d) TA1418 baddeleyite
50μm
7
8
9
12
13
1868 ± 10
1714 ± 8
1719 ± 25
1713 ± 5
1716 ± 6
spot 7
Mean = 1713 ± 4 Ma
15 points MSWD = 0.6
Isochron age
= 1715 ± 3 Ma
MSWD = 2.1
e) TA1103 baddeleyite
50μm
1
3
12
22
23
1717 ± 6
1712 ± 10
1715 ± 13
1710 ± 4
1729 ± 9
Mean = 1715 ± 4 Ma
All 23 points,MSWD = 1.4
Intercepts at
1724 ± 8 Ma
MSWD = 1.13
f) LWS130 baddeleyite
50μm
1
8
9
10
16
1682 ± 48
1701 ± 47
1715 ± 10
1714 ± 29
1715 ± 8
spot 8
spot 10
spot 1
Mean = 1716 ± 5 Ma
15 points,MSWD = 0.35
Isochron age
= 1718 ± 6 Ma
MSWD = 1.4
$^{206}Pb/^{238}U$
$^{207}Pb/^{235}U$
$^{207}Pb/^{206}Pb$
$^{204}Pb/^{206}Pb$

Guangzhou with an analytical precision ±5%. Whole-rock trace elemental compositions, including REEs, were measured using a Perkin-Elmer Sciex ELAN DRC-e ICP-MS at the State Key Laboratory of Ore Deposit Geochemistry (SKLOG), Institute of Geochemistry of CAS after closed-beaker digestion with a mixture of HF and HNO3 in Teflon bombs (Qi et al., 2000). Rh was used as an internal standard. The international standards GBPG-1, OU-6, and the Chinese National standards GSR-1 and GSR-3, were used as reference materials. The analytical precision was better than 10%. Major and trace element compositions for the mafic rocks in Huili–Dongchuan are presented in Supplementary Table S2.

Samples for Nd isotopic analysis were spiked and dissolved with HF + HNO_3 acid in Teflon bombs. Sm and Nd were separated by conventional cation-exchange techniques. The isotopic measurements were performed on a Thermal Ionization Mass Spectrometry (TIMS) - Triton at the SKLODG and a Finnigan MAT262 multi-collector mass spectrometer at the Laboratory for Radiogenic Isotope Geochemistry, Institute of Geology and Geophysics, CAS. The $^{143}Nd/^{144}Nd$ values of BCR-2 determined by TIMS during this study were 0.512513 ± 0.000004 (2σ). The $^{143}Nd/^{144}Nd$ ratios of JNDI-1 were measured as 0.512098 ± 0.000002 (2σ) by TIMS and 0.512142 ± 0.000010 (2σ) by MAT262, respectively. Nd isotopic compositions for the mafic rocks in Huili-Dongchuan are presented in Supplementary Table S2.

4. Results

4.1. U-Pb zircon and baddeleyite geochronology

4.1.1. 1.72–1.71 Ga intrusions

Zircons from sample TST1305 (diabase intruding the Tong'an Group) and BK1102 (gabbro intruding the Dongchuan Group) gave ages of >1.71 Ga (Supplementary Table S1). The zircons are simple prismatic crystals 50–120 μm in length, have aspect ratios of 1:1 to 2:1, and show obvious zoning under CL (Fig. 5a and b). Eleven analyses that were conducted on 12 zircon grains from sample TST1305 yielded a discordia line with an upper intercept age of 1714 ± 16 Ma and a lower intercept age of 277 ± 41 Ma (2σ, MSWD = 2.5) (Fig. 5a), the latter probably reflecting a late-stage thermal disturbance (the Permian Emeishan plume event? Xu et al., 2004) that also effected the 1494 ± 6 Ma gabbroic samples reported by Fan et al. (2013). All 15 measurements on zircon grains from sample BK1102 are concordant with a weighted mean $^{207}Pb/^{206}Pb$ age of 1714 ± 6 Ma (2σ, MSWD = 1.8) (Fig. 5b).

Baddeleyite grains from gabbro sample TA1103 and dike samples TST1305 and TA1418, all of which intrude the Tong'an Group, as well as grains from sample LWS1301 from a dike intruding the Dongchuan Group, are mostly anhedral, ranging from 30 to 150 μm in length, and have aspect ratios between 1:1 and 2:1 (Fig. 5c–f). Analyses of grains from dike samples TST1305, TA1418 and LWS1301 gave weighted mean $^{207}Pb/^{206}Pb$ ages of 1715 ± 4 Ma (2σ, MSWD = 0.9), 1713 ± 4 Ma (2σ, MSWD = 0.6) and 1716 ± 5 Ma (2σ, MSWD = 0.35), respectively, which are consistent with their zircon U-Pb ages within error (Fig. 5c–f). All 23 measurements on baddeleyite grains from gabbro sample TA1103 yielded a weighted mean $^{207}Pb/^{206}Pb$ age of 1715 ± 4 Ma (2σ, MSWD = 1.4). Therefore, all of our new zircon and baddeleyite U-Pb ages effectively constrain the crystallization age of these gabbros and diabase dikes to 1.72–1.71 Ga.

4.1.2. 1.70 Ga intrusions

Zircons from samples of diabase porphyry (TA1440) and gabbro (TA1444 and 13TA09) that intrude the Tong'an Group yielded ages of ~1.70 Ga (Supplementary Table S1). These zircons are clear, simple prismatic crystals without obvious zoning under CL, and they measure 80–180 μm in length with aspect ratios between 1:1 and 2:1 (Fig. 6a–c). All 15 measurements on zircon grains from sample TA1444 gave a weighted mean $^{207}Pb/^{206}Pb$ age of 1700 ± 8 Ma (2σ, MSWD = 1.2) (Fig. 6a). Most analyses on zircon grains from samples TA1440 and 13TA09 yielded concordant ages except for 2 grains from sample TA1440 and 1 grain from sample 13TA09 that are discordant due to the loss of radiogenic lead (Fig. 6b and c). Seventeen of nineteen analyses of sample TA1440 yielded a weighted mean $^{207}Pb/^{206}Pb$ age of 1700 ± 3 Ma (2σ, MSWD = 1.6) (Fig. 6b), and fifteen of sixteen analyses of sample 13TA09 gave consistent $^{207}Pb/^{206}Pb$ ratios within errors, yielding a weighted mean $^{207}Pb/^{206}Pb$ age of 1705 ± 7 Ma (2σ, MSWD = 6.5) (Fig. 6c). Therefore, the mafic gabbros and the diabase-porphyrite of this group were all emplaced at ca. 1700 Ma.

4.1.3. 1.52–1.50 Ga intrusions

Baddeleyite grains from sample RZS1301 collected from a mafic dike that intrudes the Dongchuan Group are mostly anhedral, rang from 80 to 150 μm in length, and have aspect ratios between 1:1 and 2:1 (Fig. 7a). All 21 analyses gave a $^{207}Pb/^{206}Pb$ isochron ages of 1526 ± 5 Ma (2σ, MSWD = 2.5), with a weighted mean $^{207}Pb/^{206}Pb$ age of 1519 ± 4 Ma (2σ, MSWD = 0.74) based on 18 grains that have consistent $^{207}Pb/^{206}Pb$ ratio within errors (Fig. 7a).

Zircons grains from sample 13TA43 collected from a gabbroic intrusion that intrudes the Tong'an Group are simple prismatic crystals without obvious zoning under CL, and they measure 80–120 μm in length with aspect ratios between 1:1 and 2:1 (Fig. 7b). Fourteen analyses were conducted on 14 zircon grains, yielded a discordia line with an upper intercept age of 1505 ± 16 Ma and a lower intercept age of 210 ± 52 Ma (2σ, MSWD = 3.3) with a weighted mean $^{207}Pb/^{206}Pb$ age of 1504 ± 11 Ma (2σ, MSWD = 3.3) for the four grains that have consistent $^{207}Pb/^{206}Pb$ ratios within errors (Fig. 7b).

4.2. Geochemical and Nd isotopic characteristics

The Huili-Dongchuan mafic rocks display variable whole-rock major and trace elemental contents (Supplementary Table S2). The rocks have undergone various degrees of alteration, as judged from petrographic observation and their variable LOI values. Although correlations between major oxides and MgO contents for the samples within each group (Fig. 8) suggest that the effects of alteration were negligible, we nevertheless recalculated the sums of major element oxides to 100% volatile free values. The contents of incompatible elements such as Ba, Rb, and Sr may have been modified during alteration. However, immobile elements such as the REEs, HFSEs, Th, Zr. and Ti in the Huili-Dongchuan rocks were not substantially affected by secondary alteration, as can be seen from the parallel REE and multi-element patterns (Fig. 9) and strongly correlation with Zr (not shown), and emphasis is placed on these immobile elements and Nd isotopes in the discussion below.

Mafic rocks in each group exhibit similar compositions but with some variable geochemical features. Samples from the 1.72–1.71 Ga group have the highest but most variable MgO, CaO, Al_2O_3, Cr and Ni contents of the three groups (Fig. 8, Supplementary Table S2). In contrast, Fe_2O_3, TiO_2, and total alkalis (Na_2O + K_2O) contents are commonly much lower in the 1.72–1.71 Ga group. In Fenner diagrams, the major oxides and trace elements Cr and Ni from the 1.70 and 1.52–1.50 Ga groups show similar evolutionary trends except for the relatively consistent Al_2O_3 and CaO contents in the 1.52–1.50 Ga group (Fig. 8). In the rock classification diagrams, samples from the

Fig. 5. Zircon and baddeleyite U-Pb Concordia diagrams with transmitted CL images of representative zircon grains and backscattered electron images of representative baddeleyite grains from the 1.72–1.71 Ga group. Mean ages represent weighted mean $^{207}Pb/^{206}Pb$ ages with 95% confidence intervals (2σ), which were calculated without those spots with pink circles. Red circles on zircon/baddeleyite grains indicate the U-Pb dating positions. Age of each spot is presented as $^{207}Pb/^{206}Pb$ age (2σ).

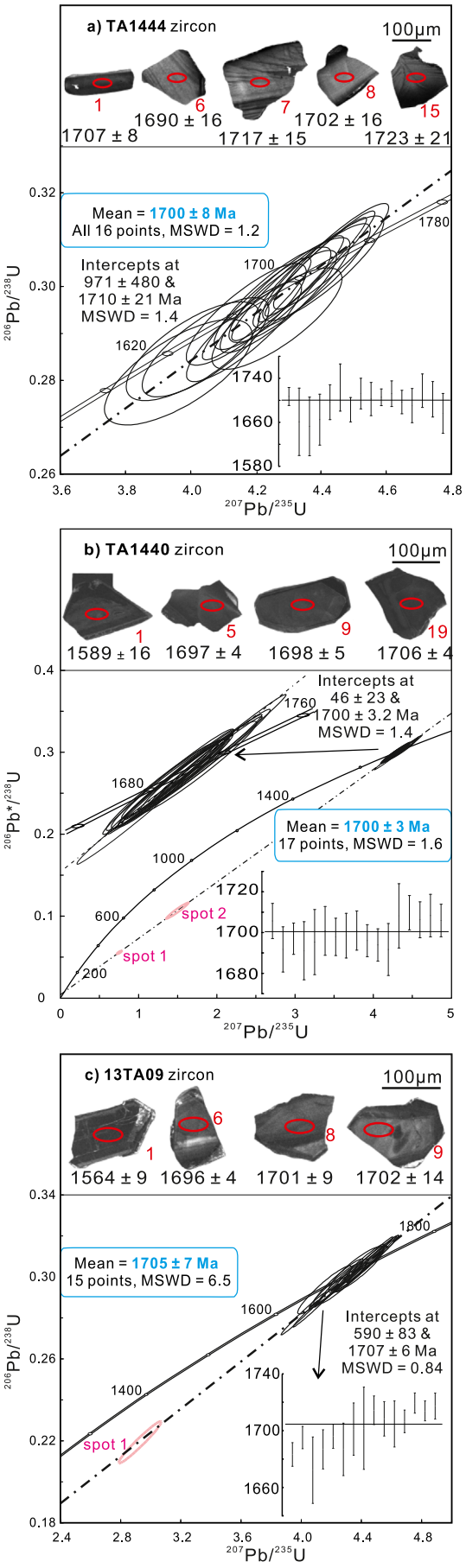

Fig. 6. Zircon and baddeleyite U-Pb concordia diagrams with transmitted CL images of representative zircon grains and backscattered electron images of representative baddeleyite grains from the 1.70 Ga group. Mean ages represent weighted mean $^{207}Pb/^{206}Pb$ ages with 95% confidence intervals (2σ), which were calculated without those spots with pink circles. Red circles on zircon/baddeleyite grains indicate the U-Pb dating positions. Age of each spot is presented as $^{207}Pb/^{206}Pb$ age (2σ).

1.70 Ga and 1.52–1.50 Ga groups plot in the alkaline field, whereas the 1.72–1.71 Ga samples plot in the tholeiitic basalt field (Fig. 10).

Samples from the 1.70 Ga and 1.52–1.50 Ga groups have parallel REE patterns with enrichments in light rare earth elements and "humped" primitive mantle-normalized multi-element patterns that show variable enrichment in all incompatible elements but with no obvious Nb-Ta anomalies relative to the neighboring elements (Fig. 9). These characteristics are similar to typical intraplate alkali basaltic rocks in CFB and OIB provinces (Sun and McDonough, 1989) (Fig. 10). In contrast, the 1.72–1.71 Ga group samples display relative flat REE patterns and primitive mantle-normalized multi-element patterns similar to those of typical E-MORB (Sun and McDonough, 1989) (Fig. 9).

The Sm-Nd isotopic compositions show limited variations between samples from each group of mafic rocks in the Huili-Dongchuan area (Supplementary Table S2). The 1.72–1.71 Ga samples have $(^{143}Nd/^{144}Nd)_i$ ratios that rang from 0.510426 to 0.510590, ε_{Nd} (T) values that rang from 0.12 to 3.34. The 1.70 Ga group samples show the least variability in their $(^{143}Nd/^{144}Nd)_i$ ratios (0.510600 to 0.510706 with one exception of 0.510439), and the corresponding ε_{Nd} (T) values rang from 3.16 to 5.24. The 1.52–1.50 Ga group samples have $(^{143}Nd/^{144}Nd)_i$ ratios ranging from 0.510573 to 0.510724 and ε_{Nd} (T) values ranging from −2.55 to 0.50.

5. Discussion

5.1. Chronological and stratigraphic differences between the Huili and Tong'an groups

Zircons from mafic rocks in the Huili-Dongchuan area are clearly magmatic, as judged from their CL images and Th/U ratios (Figs. 5–7; Supplementary Table S1), and together with baddeleyites, which have a very stable U-Pb isotopic system in mafic–ultramafic rocks (e.g., Li et al., 2010), the age data for these minerals suggest that these gabbroic intrusions and dikes formed in three time intervals of 1.72–1.71, 1.70, and 1.52–1.50 Ga (Figs. 2c and 5–7; Supplementary Table S1).

The Tong'an Group was previously suggested to be a part of the Huili Group (Fig. 2a and b). However, the 1.72–1.50 Ga mafic rocks that intrude the Heishan and Qinglongshan formations effectively constrain the depositional age of the Tong'an Group to >1.72 Ga, making it much older than the Huili Group which has a minimum depositional age of 1.0 Ga (Fig. 2c). Moreover, field work indicates that these two groups are in fault contact, and no continuous sequence between them has been identified so far (Figs. 2 and 3). Therefore, the Tong'an and Huili groups do not belong to the same stratigraphic group and cannot be correlated stratigraphically (Fig. 2c). Our new data, on the other hand, support the subdivision of the Dongchuan and Kunyang groups by previous workers (e.g., Li et al., 1988; Wu et al., 1990; Zhao et al., 2010) (Fig. 2c). We thus suggest the Tong'an, Dongchuan and Hekou groups to be stratigraphically correlatable units (Fig. 2c).

5.2. Petrogenesis of the 1.72–1.50 Ga mafic rocks

5.2.1. Differentiation processes and crustal contamination

The variations in SiO_2 and MgO contents within each series of the Huili–Dongchuan mafic magmatic rocks point to the effects of pronounced fractional crystallization (FC) (Fig. 8). In the 1.72–1.71 Ga group, the Yinmin and Tong'an diabase dikes show the smallest influence of FC as they have the highest and relatively stable MgO contents

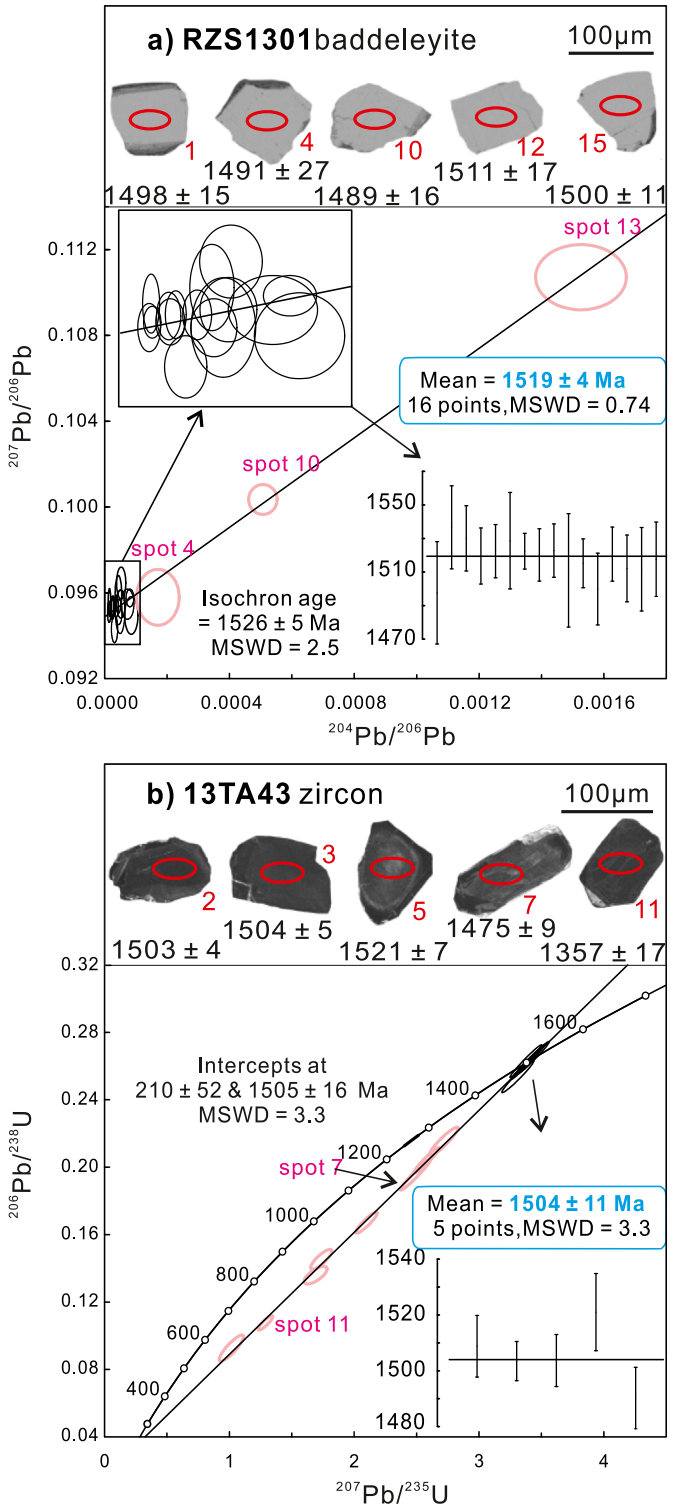

Fig. 7. Zircon and baddeleyite U-Pb concordia diagrams with transmitted CL images of representative zircon grains and backscattered electron images of representative baddeleyite grains from the 1.52–1.50 Ga group. Mean ages represent weighted mean $^{207}Pb/^{206}Pb$ ages with 95% confidence intervals (2σ), which were calculated without those spots with pink circles. Red circles on zircon/baddeleyite grains indicate the U-Pb dating positions. Age of each spot is presented as $^{207}Pb/^{206}Pb$ age (2σ).

(Fig. 8), which is consistent with the fractionation trends indicated by trace element correlation diagrams (Supplementary Fig. S1). Fractional crystallization of clinopyroxene and plagioclase and accumulation of Fe-Ti oxides (magnetite and ilmenite) appear to have played major roles in modifying the compositional evolution of the other 1.72–1.71 Ga mafic rocks, and the compositional variations within these diabase dikes and gabbros can be readily explained by FC and accumulation processes. For example, the decreases in Al_2O_3 and CaO with decreasing MgO contents (Fig. 8) are likely to have resulted from clinopyroxene fractionation, whereas the increases in Fe_2O_3 and TiO_2 with decreasing MgO contents were due to the accumulation of Fe-Ti oxides. Moreover, the trace element correlation diagrams (Supplementary Fig. S1) also suggest significant separation/addition of clinopyroxene, plagioclase and magnetite.

In the 1.70 Ga and 1.52–1.50 Ga groups, the 1.70 Ga diabase porphyry and the 1.50 Ga gabbro have the highest and relatively stable MgO contents, reflecting a process of *in-suit* crystallization (Fig. 8). However, fenner diagrams and the trace element correlation diagrams involve V, Cr, Ni, Zr and Y suggest fractional crystallization of clinopyroxene have significantly modified the chemical compositions of the other rocks from the two groups (Supplementary Fig. S1). The crystallization and removal of Fe-Ti oxides appear to have controlled the variation in chemical compositions as Fe_2O_3 and TiO_2 decrease with decreasing MgO contents (Fig. 8), as also shown by the positive correlations of Cr and Ni with MgO contents (Fig. 8) as the compatible behavior of Cr and Ni in magnetite. The relatively consistent CaO and slight increase in Al_2O_3 and $K_2O + Na_2O$ contents with decreasing MgO contents (Fig. 8) imply that plagioclase was not the main fractional mineral. The involvement of FC processes is also shown by variable Nb/La ratios but relatively stable $\varepsilon_{Nd}(T)$ values and Nb/Th ratios for samples of the 1.70 Ga and 1.52–1.50 Ga groups (Fig. 11).

The absence of significant depletions in Nb and Ta relative to elements of similar incompatibility suggests negligible contamination in the magma channels during crystallization of the Huili-Dongchuan rocks (Fig. 9). However, in the 1.72–1.71 group, the samples with relatively low $\varepsilon_{Nd}(T)$ values generally have lower MgO contents and Th/Nb ratios but higher Nb/La ratios (Fig. 11; Supplementary Fig. S2), suggesting that the possible assimilation and fractional crystallization (AFC) processes could have occurred during cooling and crystallization of the parental magma.

Here, we present possible models of crystallization processes for each of the three groups of mafic rocks based on the above assessment of the roles played by various fractionating minerals (Supplementary Fig. S3). The fact that our modeling calculations fit well with most trace element and REE patterns for the samples, indicates that the FC and AFC processes were important in modifying the chemical compositions of these rocks.

5.2.2. Mantle source

Geochemical distinctions can be made among the 1.72–1.50 Ga mafic rocks of the Huili-Dongchuan area on the basis of their major- and trace-element compositions. For example, in an $(Na_2O + K_2O)$ vs. SiO_2 classification diagram, the 1.72–1.71 Ga samples plot in the field of tholeiitic basaltic rocks, whereas the 1.70 and 1.52–1.50 Ga samples plot in the alkaline field (Fig. 10). Furthermore, the 1.72–1.71 Ga samples show *E*-MORB-like REE and trace element characteristics, whereas the 1.70 Ga and 1.52–1.50 Ga samples display REE patterns and multi-element spidergrams similar to those of OIB-type basalts (Fig. 9). Together with the variations in their Nd isotope contents, these data suggest that the rocks originated from a heterogeneous mantle source, with the distinctive geochemical characteristics having been generated by varying degrees of crustal assimilation/magma mixing, or varying degrees of partial melting. However, the exact source compositions are hard to be constrained due to their cumulate nature and the significant alteration on these rocks. Moreover, there are no chilled margins that can be used for estimating parental magma compositions. Therefore, in this study, we try to estimate their source characteristics and melting conditions by using of the trace element and Nd isotopic compositions of the Huili-Dongchuan mafic rocks (Aldanmaz et al., 2000).

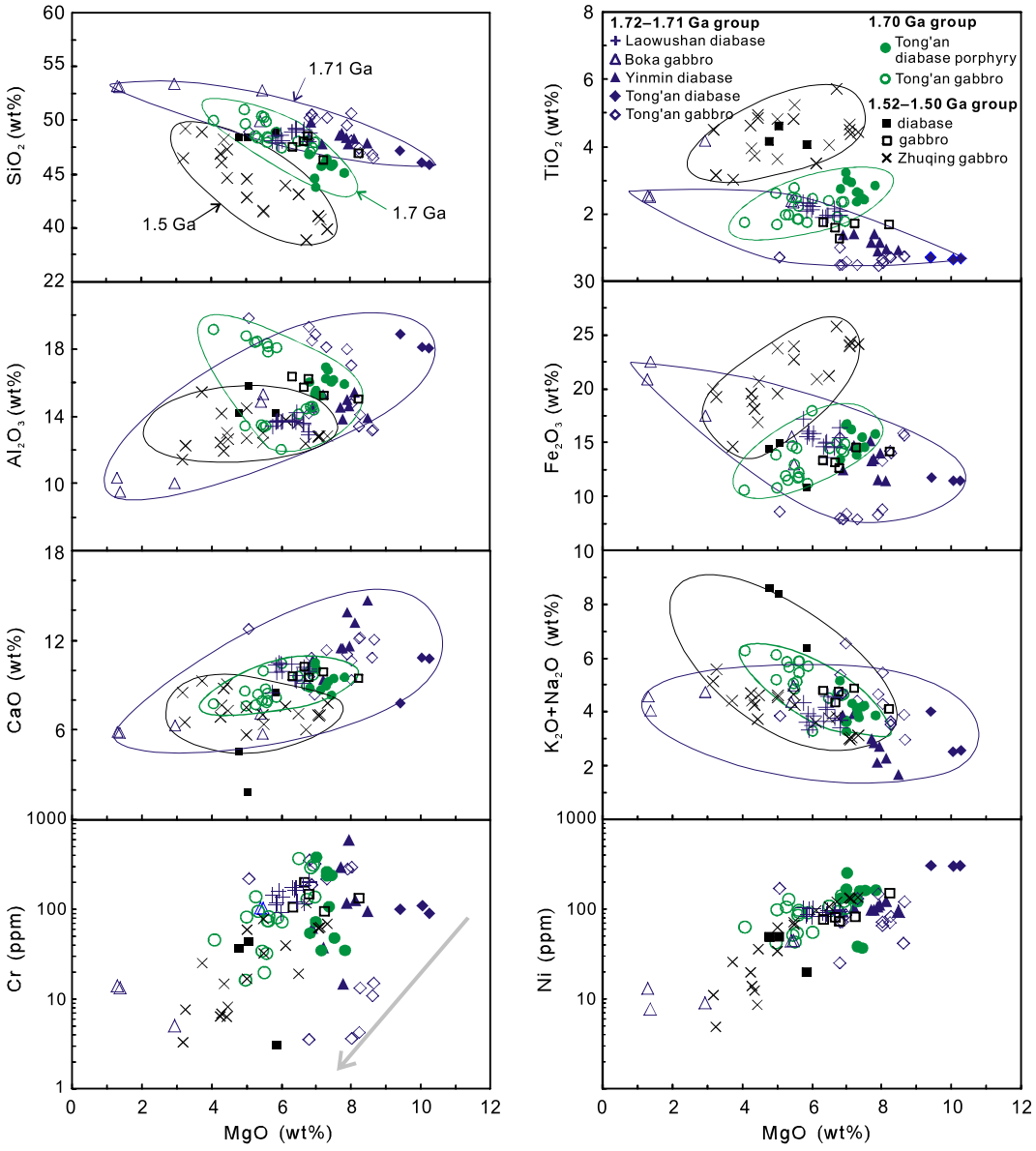

Fig. 8. Fenner diagrams for the mafic rocks in the Huili–Dongchuan area.

The Nb/Th ratios decrease substantially from the 1.70 Ga rocks to the 1.72–1.71 Ga group and from the rocks of 1.72–1.71 Ga group to those of the 1.52–1.50 Ga group, and so do the $\varepsilon_{Nd}(T)$ values (Fig. 11). This could be due to the influence of an enriched component in the melts, which would have lowered their Nb/La and Nb/Th ratios and $\varepsilon_{Nd}(T)$ values. The 1.70 Ga rocks show the smallest influence of the enriched component, and they display trace element patterns similar to those of OIB (Fig. 9) with $\varepsilon_{Nd}(t)$ values varying between +3.16 and + 5.24, suggesting generation by low-degree partial melting of a depleted upper mantle (e.g., Xu et al., 2001). The degree of partial melting of the basaltic rocks can be estimated using their rare earth element compositions given their different geochemical behaviors in the typical mantle aluminous phases (e.g., Aldanmaz et al., 2000; and references therein). The low Gd/Yb and La/Sm ratios of the 1.72–1.71 Ga rocks indicate a higher degree of partial melting then the other two groups of rocks (Fig. 12). Moreover, the Huili-Dongchuan rocks show a diagonal trend between low-degree deep melting OIB-like compositions and high-degree shallow melting MORB-like compositions (Fig. 12). Thus, the 1.72–1.71 Ga rocks probably represent a comparatively higher degree of partial melting of an enriched mantle formed at a shallow depth, whereas the 1.70 Ga rocks and the 1.52–1.50 Ga rocks were probably produced by small-degree partial melting of a depleted asthenosphere mantle and an enriched mantle at a higher depth, respectively (Fig. 12). Notice that, the significantly low Al_2O_3/TiO_2 ratios (4.76–7.18 compared with ~20 in primitive mantle) and high $(Sm/Yb)_{PM}$ ratios (2.87–3.35) of the 1.70 Ga rocks indicate a quite low degree of partial melting (Fig. 12b). The modeled degree of melting for the 1.70 Ga rocks is calculated to be 2% (Supplementary Fig. S4). It is generally known that, a degree of melting substantially <1% is considered unlikely because of the difficulty of extracting such small amounts of melt from the source rock owing to surface forces that inhibit magma segregation until appreciable extents of melting (≥1%) have been achieved (Richter and McKenzie, 1984; Ribe, 1988). It has been suggested that high-Ti mafic rocks were generated by the Emeishan large igneous province as the result of 1.5% partial melting of the mantle (Xu et al., 2001). Moreover, a starting composition calculated based on 2% degree of partial melting can generated melts with trace element and REE patterns similar to that of 1.70 Ga samples (Supplementary Fig. S3). Therefore, the

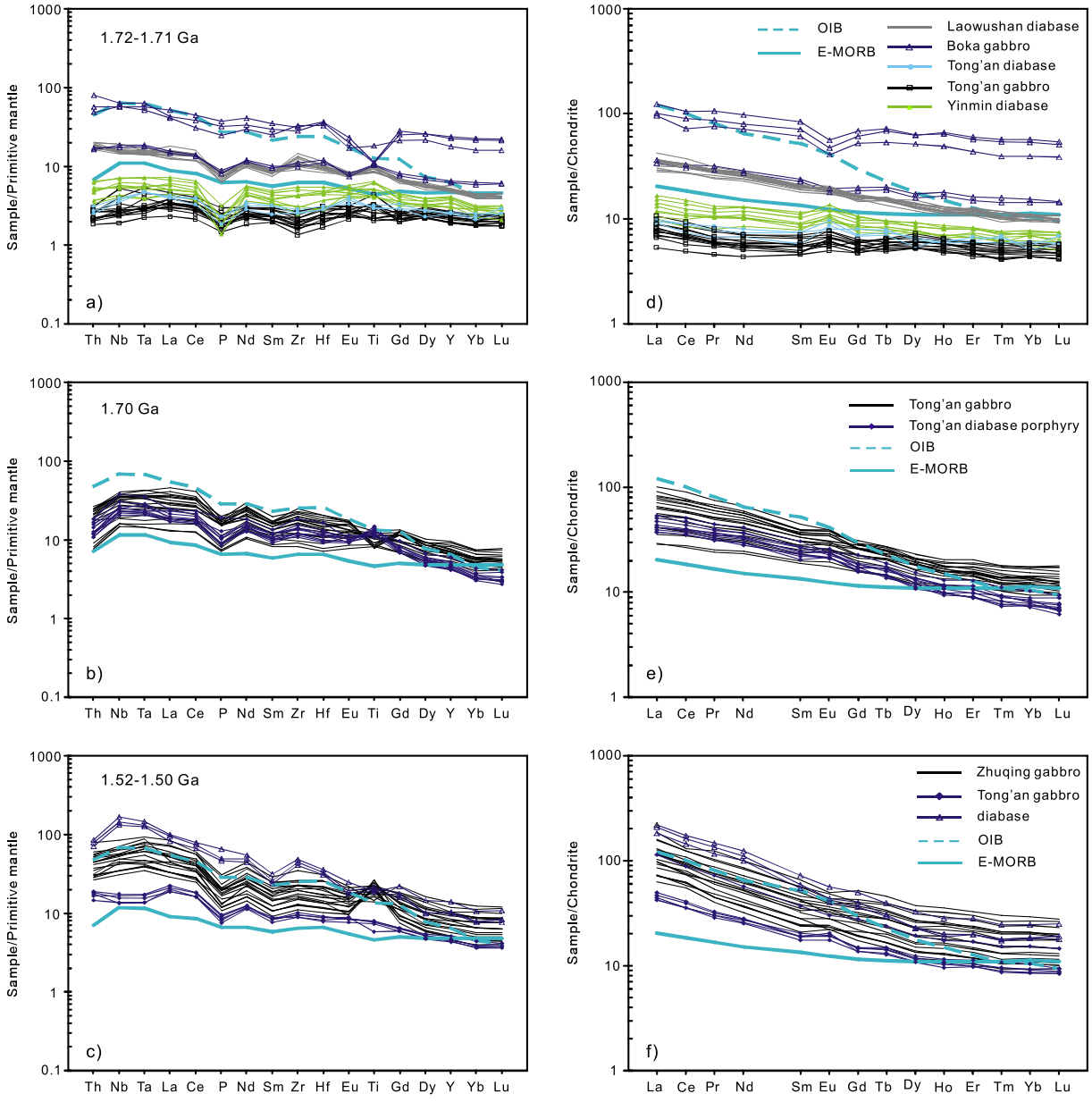

Fig. 9. Primitive mantle-normalized incompatible trace element spider diagrams for samples from a) the 1.72–1.70 Ga group, b) the 1.70 Ga group and c) the 1.52–1.50 Ga group, respectively, and Chondrite-normalized REE patterns for these rocks (d–f). Chondrite-normalizing values are from Boynton (1984). Primitive mantle-normalizing values, and OIB and E–MORB data are from Sun and McDonough (1989).

1.70 Ga rocks were probably generated by a simple one-stage melting of asthenosphere mantle with a DMM-like composition at a depth of 200–400 km (after Wyllie, 1981). In contrast, the 1.72–1.71 Ga and 1.52–1.50 Ga rocks require enrichment of the asthenosphere to explain their mantle source characteristics as they reflect mixing of depleted mantle and an enriched component (Fig. 11).

The lack of depletion in Nb and Ta in our sample rules out the possibility of involvement of the continental crustal material and SCLM as they are too depleted in Nb and Ta relative to elements of similar incompatibility. Dikes and veins with enriched compositions that are emplaced in a depleted upper mantle provide a possible way of creating an enriched mantle component (Niu et al., 2002), which, however, unlikely to produce such large volume of basaltic rocks with such a uniform geochemistry over a broad area such as Huili-Dongchuan (Fig. 3). The enriched signatures of many continental and oceanic intraplate alkaline rocks have been also suggested to be generated by a lower mantle-derived plume component in the source region (e.g., Wilson, 1993). In this scenario, relatively enriched component, such as material from recycled oceanic crust, from deep in the lower mantle (including the core/mantle boundary) rise adiabatically up to asthenosphere depths and generate enriched heterogeneities within the mantle that can then produce rocks with an OIB signature (e.g., Hofmann and White, 1982; Hart, 1988). Future study will provide more insights about the exact nature and origin of the enriched component that is required to produce the 1.72–1.71 Ga and 1.52–1.50 Ga rocks.

5.3. A plume associated genesis and geological implications

The estimated general characteristics of the primary magma for the 1.72–1.70 Ga mafic rocks in the Huili-Dongchuan area suggest varying degrees of partial melting of a metasomatized and heterogeneous asthenospheric mantle, with a decrease in melt fraction over time (from 1.72 Ga to 1.70 Ga) (Fig. 12). Such a temporal trend is consistent with the involvement of a mantle plume (or plumes) in the generation of

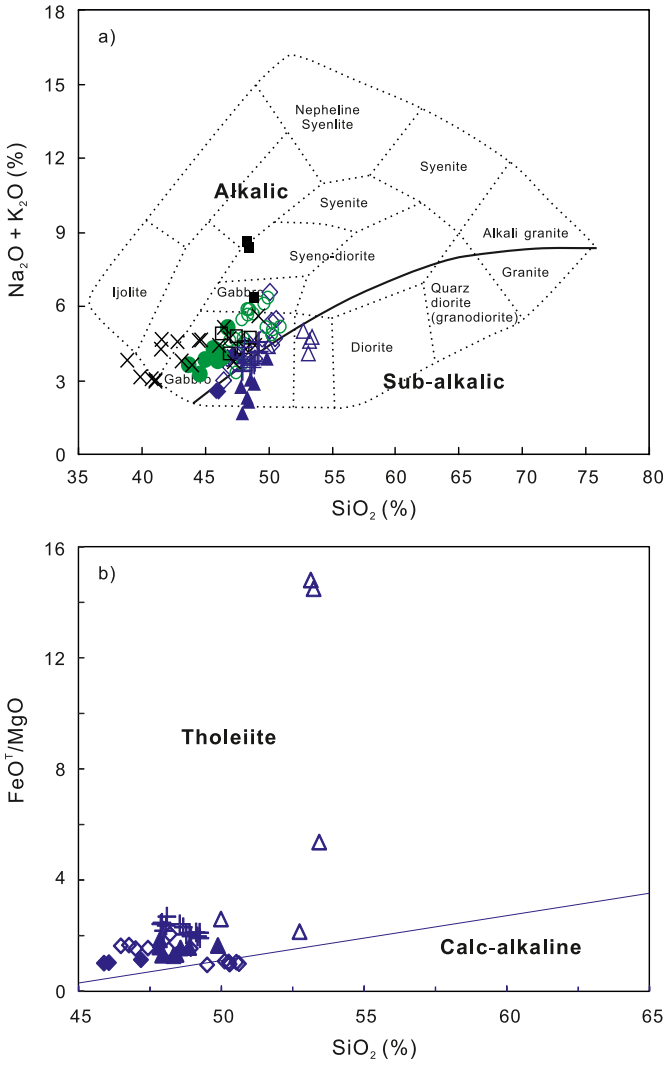

Fig. 10. Plots of ($Na_2O + K_2O$) and FeO^T/MgO vs. SiO_2, modified after Miyashiro (1974) and Cox et al. (1979), for classification of the mafic rocks in the Huili–Dongchuan area. Symbols as in Fig. 8.

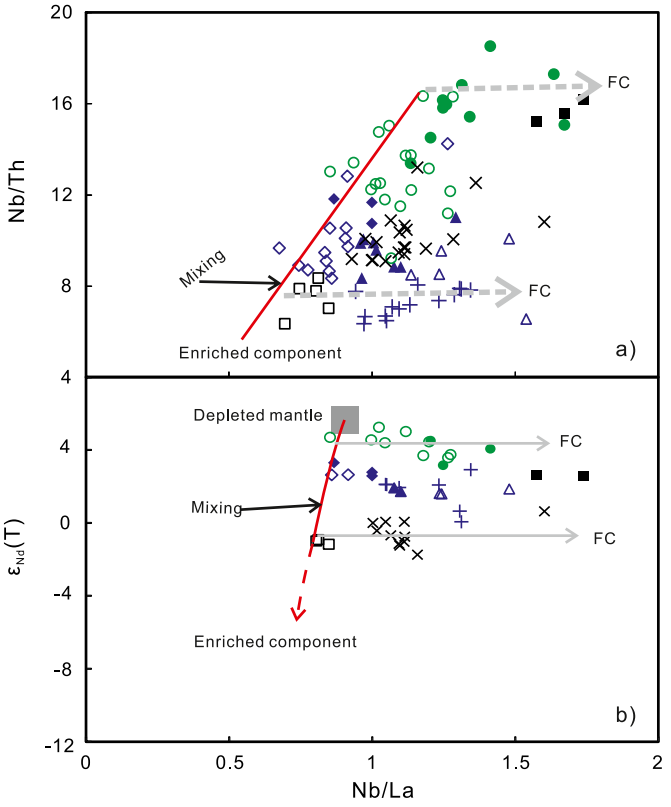

Fig. 11. Plots of a) Nb/Th vs. Nb/La and b) $\varepsilon_{Nd}(T)$ vs. Nb/La for studied mafic rocks from the mafic rocks in the Huili–Dongchuan area. Partition coefficients used for the modeling are from GERM Partition Coefficients Database (https://earthref.org/). Cpx = clinopyroxene, Pl = plagioclase, Mt. = magnetite. $\varepsilon_{Nd}(T)$ were calculated using the age of 1700 Ma. Symbols as in Fig. 8.

melt, meaning that the primary magma for the 1.72–1.71 Ga rocks could have been a melt from the metasomatized asthenosphere directly above the plume head at a shallow depth, whereas the 1.70 Ga rocks could have been generated by the plume tail at a greater depth (Figs. 12 and 13). The 1.52–1.50 Ga rocks could represent later magmatic activities that induced the partial melting of a mantle which had already been metasomatized by plume-derived melts with enriched components during 1.72–1.70 Ga (Fig. 13). We note that the rocks generated by the 1.72–1.71 Ga activity are the most widespread in the Huili–Dongchuan area and that the 1.70 Ga generation rocks are scarcely distributed (Fig. 3). This is consistent with observation that the magma associated with a plume tail is commonly significantly less voluminous than that associated with the plume head.

A mantle plume-related genetic model can also explain the very minor amount of crustal contamination in the 1.70 rocks, as experimental and numerical modeling studies have shown that a plume head may carry large amounts of surrounding materials (such as lithospheric materials), whereas a plume tail typically entrains little of surrounding materials as temperature decreases and buoyancy increases (e.g., Hauri et al., 1994). Moreover, the ascending channel for the 1.70 Ga magmas would have been unobstructed owing to the prior removal of materials by the plume head, which would have allowed magma to arise more rapidly without any pronounced involvement of crustal materials, in contrast to the 1.72–1.71 Ga rocks. In addition, the fact that the 1.72–1.71 Ga samples have an *E*-MORB-like REE and trace element characteristics, whereas the 1.70 Ga samples have OIB-like REE patterns and multi-element spidergrams also suggests a close affinity to a plume origin. This pattern is similar to that observed on the Hawaiian Islands, where an OIB-like magma comes after an E-MORB-like magma (e.g., Wyllie, 1988).

The lower Heishan Formation consists of sandstones interbedded with shale, whereas the middle part of the formation consists of carbonaceous slates, and the upper part dolostone with interlayers of slate, which indicates a rise in sea level in this region prior to 1.70 Ga (Fig. 2c). This rise was followed by a further sustained rise in sea level until the deposition of dolostones of the Qinglongshan Formation and the deep-water volcanic sedimentary series of the Tangtang Formation that overlies the Qinglongshan Formation (Pang et al., 2015). The Dongchuan Group also features indicative of a complete sedimentary record from alluvial fan and fluvial system to deep water marine basin during the period 1.7–1.5 Ga (Wang and Zhou, 2014), which is typical of sedimentation in a continental rifting setting. Moreover, the 1.7 Ga rocks have REE patterns and multi-element spidergrams similar to those of modern basalts identified in continental rifts (e.g., Ritter et al., 2001). Furthermore, the metasedimentary and metavolcanic rocks in the correlatable stratigraphic units are similar to sedimentation in a continental rifting setting (Li et al., 1988; Wu et al., 1990; Zhao et al., 2010; Chen et al., 2013, Wang and Zhou, 2014; Wang et al., 2014). All of the above suggests that the rift basin at the Huili-Dongchuan area was probably part of a ~ 1.7 Ga N–S-trending rift basin in the Kangdian region near the southwestern margin of the Yangtze Block (Fig. 1), which could have been induced by a Paleoproterozoic mantle plume.

Late Paleo- to Mesoproterozoic anorogenic magmatism associated with the break-up of the supercontinent Nuna have generally been

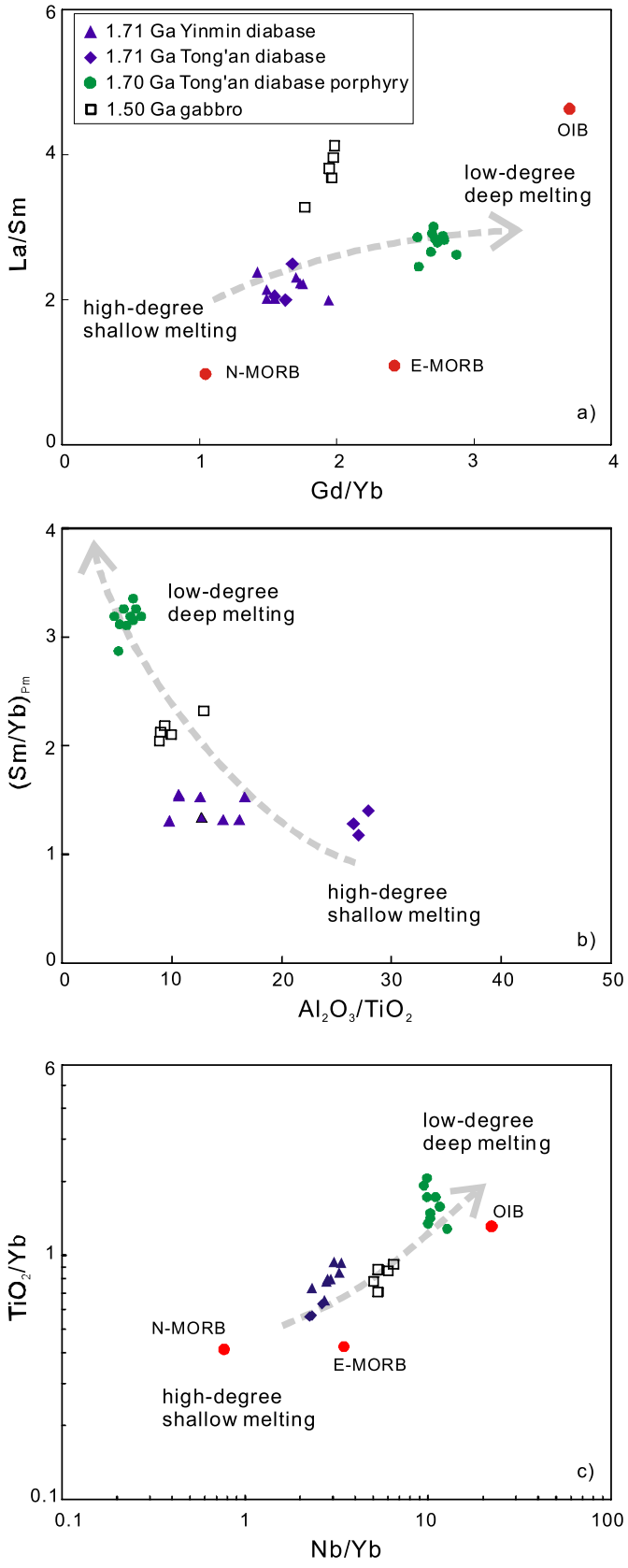

Fig. 12. Plots of a) La/Sm vs. Gd/Yb, b) $(Sm/Yb)_{Pm}$ vs. Al_2O_3/TiO_2, and c) TiO_2/Yb vs. Nb/Yb for samples of the mafic rocks in the Huili–Dongchuan area showing the nature and origin of the parental magmas and mantle process. Samples from intrusions that have experienced significant FC and AFC processes are excluded from these diagrams. Only samples collected from the 1.72–1.71 Ga Yinmin and Tong'an diabase dikes, the 1.70 Ga Tong'an diabase-porphyrite and the 1.52–1.50 Ga gabbro are shown here. N-MORB, E–MORB and OIB data are taken from Sun and McDonough (1989).

linked to mantle plume activity (e.g., Meert and Santosh, 2017; and references therein). Thus, the ~1.7 Ga magmatism occurred in the southwestern Yangtze Block were likely a part of them. The precise position and role of the Yangtze Block in the assembly and break-up of the supercontinent Nuna require further investigation especially on paleomagnetic data which is unavailable so far. However, further research works such as the identification of magmatic events comparable to that reported in this study will provide important constraints for linking the Yangtze Block to other cratons that were once parts of the supercontinent.

6. Conclusions

We report results of detailed geochronological and geochemical analyses on newly discovered Paleo- to early Mesoproterozoic diabase dikes and gabbroic and diabase-porphyrite plutons in southwestern Yangtze Block, South China. Precise SIMS zircon and baddeleyite U-Pb dating provide first evidence for three episodes of mafic rocks between 1.72 and 1.50 Ga in southwestern Yangtze Block. These ages constraint the initial depositional age of the previously poorly dated Tong'an and Dongchuan groups to >1.72 Ga. On the basis of chemical compositions and isotopic characteristics of these mafic rocks, a metasomatized and heterogeneous mantle source is inferred. Our modeling shows that the primary magma for the 1.72–1.71 Ga rocks was likely generated by high-degree partial melting of metasomatized asthenospheric mantle above a plume head at a shallow depth, whereas the 1.70 Ga rocks could have derived by low-degree partial melting of the asthenosphere mantle triggered by the plume tail. The 1.52–1.50 Ga rocks represent subsequent magmatic events involving low-degree partial melting of previously metasomatized asthenosphere mantle, with plume-derived component providing the greatest amount of enrichment, as indicated by the trace element and Nd isotopic signatures of the 1.52–1.50 Ga rocks. Model calculations suggest that FC and AFC were the most important processes to have modified the chemical compositions of these rocks during cooling of their parental magmas. The Huili-Dongchuan area was probably part of a ~ 1.7 Ga N-S-trending rift basin near the southwestern margin of the Yangtze Block, and the rifting could have been induced by a Paleoproterozoic mantle plume.

Supplementary data to this article can be found online at https://doi.org/10.1016/j.gr.2020.06.019.

CRediT authorship contribution statement

Hong-Peng Fan: Data curation, Writing - original draft. **Wei-Guang Zhu:** Supervision, Project administration, Writing - review & editing. **Zheng-Xiang Li:** Supervision, Writing - review & editing.

Declaration of competing interest

We declare that we have no financial and personal relationships with other people or organizations that can inappropriately influence our work. There is no professional or other personal interest of any nature or kind in any product, service and/or company that could be construed as influencing the position presented in or the review of the manuscript entitled.

Acknowledgements

We appreciate Q.L. Li, G.Q Tang, and X.X. Lin for their assistances in SIMS dating, J. Hu, G.P. Bao and Y. Huang for trace element analyses by ICP-MS, Z.Y. Chu, F. Xiao, and X.B. Li for Nd isotope analyses by TIMS, and Z.Y. Chu, C.F. Li and W.J. Hu for Nd isotope analyses by MAT262. The paper has benefited from constructive comments of the Editor Prof. Y.P. Dong and two anonymous reviewers. This work is supported by the

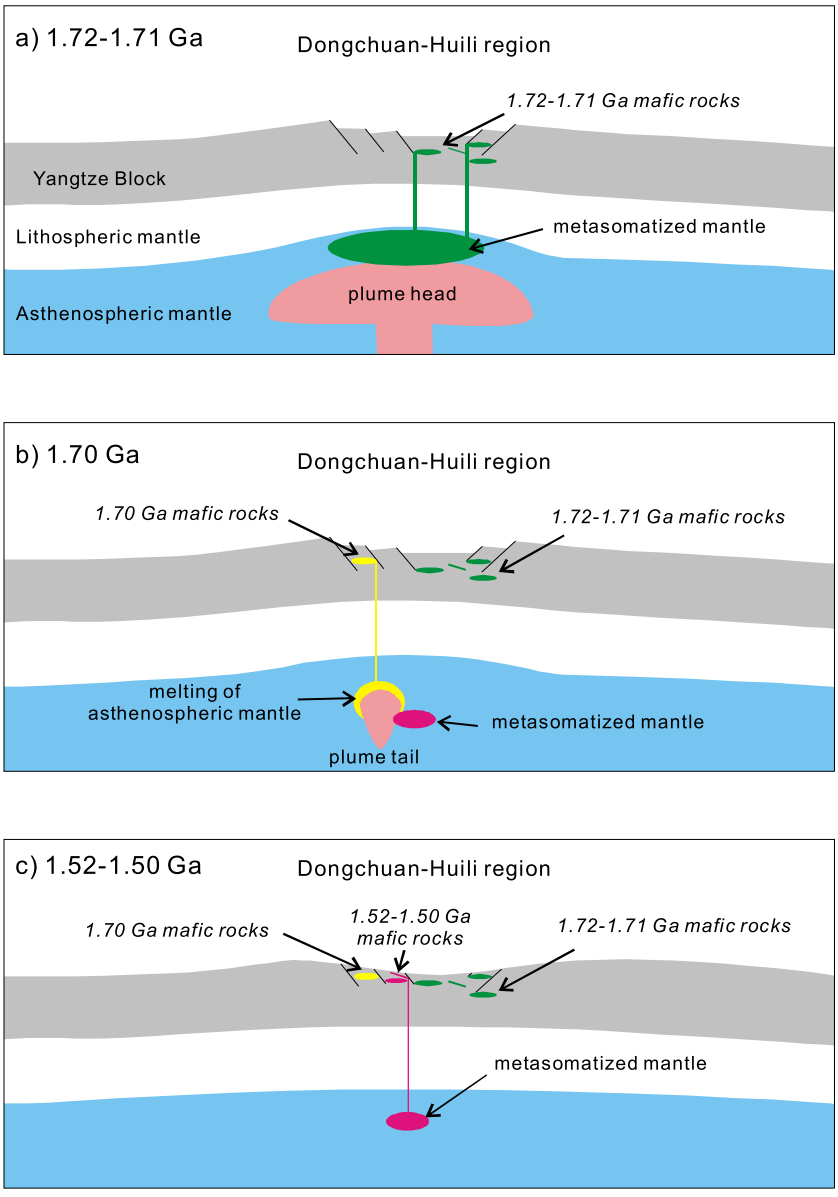

Fig. 13. Schematic images illustrating the origion of the 1.72–1.50 Ga Huili-Dongchuan mafic rocks and the tectonic evolution of southwestern Yangtze Block during late Paleo- to Mesoproterozoic. a) A Paleoproterozoic mantle plume transported enriched components from the lower mantle (including the core/mantle boundary) into the overlying upper mantle to form a metasomatized asthenosphere mantle. Subsequently, regional rifting initiated by the plume caused the elevation of the thermal boundary and induced a high-degree partial melting of the previously metasomatized asthenosphere mantle at a shallow depth to generate the 1.72–1.71 Ga *E*-MORB-like gabbroic plutons and diabase dikes. b) At 1.70 Ga, the plume tail induced the melting of the asthenosphere mantle at a greater depth, leading to the formation of the 1.70 Ga OIB-like gabbroic and diabase-porphyrite plutons. c) During theearly Mesoproterozoic, the previously metasomatized mantle underwent a low-degree partial melting at great depth to generate the 1.52–1.50 Ga OIB-like gabbroic plutons and diabase dikes.

NSFC (Grants 41572074, 41403044, and 41273049). This is contribution 1524 from the ARC Centre of Excellence for Core to Crust Fluid Systems (http://www.ccfs.mq.edu.au/).

References

Aldanmaz, E., Pearce, J.A., Thirlwall, M.F., Mitchell, J.G., 2000. Petrogenetic evolution of late Cenozoic, post-collision volcanism in western Anatolia, Turkey. J. Volcanol. Geotherm. Res. 102, 67–95.

Boynton, W.V., 1984. Geochemistry of the rare earth elements: meteorite studies. In: Henderson, P. (Ed.), Rare Earth Element Geochemistry. Elsevier, pp. 63–114.

Chen, W.T., Zhou, M.F., Zhao, X.F., 2013. Late Paleoproterozoic sedimentary and mafic rocks in the Hekou area, SW China: Implication for the reconstruction of the Yangtze Block in Columbia. Precambrian Res. 231, 61–77.

Chen, W.T., Sun, W.H., Wang, W., Zhao, J.H., Zhou, M.F., 2014. "Grenvillian" intra-plate mafic magmatism in the southwestern Yangtze Block, SW China. Precambrian Res. 242, 138–153.

Cox, K.G., Bell, J.D., Pankhurst, R.J., 1979. The Interpretation of Igneous Rocks. Allen and Unwin, London, UK. 450 pp.

Cui, X., Wang, J., Sun, Z., Wang, W., Deng, Q., Ren, G., Liao, S.Y., Huang, M.D., Chen, F.L., Ren, F., 2019. Early Paleoproterozoic (ca. 2.36 Ga) post-collisional granitoids in Yunnan, SW China: Implications for linkage between Yangtze and Laurentia in the Columbia supercontinent. J. Asian Earth Sci. 169, 308–322.

Ernst, R.E., Wingate, M.T.D., Buchan, K.L., Li, Z.X., 2008. Global record of 1600–700 Ma large Igneous Provinces (LIPs): Implications for the reconstruction of the proposed Nuna (Columbia) and Rodinia supercontinents. Precambrian Res. 160, 159–178.

Evans, D.A.D., Mitchell, R.N., 2011. Assembly and breakup of the core of Paleoproterozoic-Mesoproterozoic supercontinent Nuna. Geology 39, 443–446.

Fan, H.P., Zhu, W.G., Li, Z.X., Zhong, H., Bai, Z.J., He, D.F., Chen, C.J., Cao, C.Y., 2013. Ca. 1.5 Ga mafic magmatism in South China during the break-up of the supercontinent Nuna/Columbia: the Zhuqing Fe–Ti–V oxide ore-bearing mafic intrusions in western Yangtze Block. Lithos 168-169, 85–98.

Fan, H.P., Zhu, W.G., Zhong, H., Bai, Z.J., He, D.F., Ye, X.T., Chen, C.J., Cao, C.Y., 2014. Platinum-group element geochemistry of the Zhuqing Fe–Ti–V oxide ore-bearing mafic intrusions in western Yangtze Block, SW China: Control of platinum-group elements by magnetite. Mineral. Petrol. 109, 419–438.

Gao, L.Z., Zhang, H., Zhang, C.H., Ding, X.Z., Yin, C.Y., Wu, Z.J., Song, B., 2018. Collate and stipulate the sequences of the mesoproterozoic kunyang group in eastern Yunnan and its position in stratigraphic column of China. Geological Review 64, 283–298 (in Chinese with English abstract).

Geng, Y., Yang, C., Du, L., Wang, X., Ren, L., Zhou, X., 2007. Chronology and tectonic environment of the Tianbaoshan formation: new evidence from zircon SHRIMP U-Pb age and geochemistry. Geological Review 53, 556–563 (in Chinese with English abstract).

Greentree, M.R., Li, Z.X., 2008. The oldest known rocks in south-western China: SHRIMP U-Pb magmatic crystallization age and detrital provenance analysis of the Paleoproterozoic Dahongshan Group. J. Asian Earth Sci. 33, 289–302.

Greentree, M.R., Li, Z.X., Li, X.H., Wu, H., 2006. Late Mesoproterozoic to earliest Neoproterozoic basin record of the Sibao orogenesis in western South China and relationship to the assembly of Rodinia. Precambrian Res. 151, 79–100.

Hart, S.R., 1988. Heterogeneous mantle domains: signatures, genesis and mixing chronologies. Earth Planet. Sci. Lett. 90, 273–296.

Hauri, E.H., Whitehead, J.A., Hart, S.R., 1994. Fluid dynamic and geochemical aspects of entrainment in mantle plumes. J. Geophys. Res. 99, 275–300.

He, D.F., 2009. Petrological and Geochemical Characteristics of the Lala Copper Deposit in Sichuan Province. Unpublished Ph.D. thesis, The Gradute School of the Chinese Academy of Sciences, China, 103 pp (in Chinese with English abstract).

Hofmann, A.W., White, W.M., 1982. Mantle plumes from ancient oceanic crust. Earth Planet. Sci. Lett. 57, 421–436.

Hui, B., Dong, Y.P., Cheng, C., Long, X.P., Liu, X.M., Yang, Z., Sun, S.S., Zhang, F.F., Varga, J., 2017. Zircon U-Pb chronology, Hf isotope analysis and whole-rock geochemistry for the Neoarchean-Paleoproterozoic Yudongzi complex, northwestern margin of the Yangtze craton, China. Precambrian Res. 301, 65–85.

Li, F.H., Tan, J.M., Shen, Y.L., Yu, F.X., Zhou, G.F., Pan, X.N., Li, X.Z., 1988. The Presinian in the Kangdian Area. Chongqing Publishing House, Chongqing (396pp in Chinese).

Li, Q.L., Li, X.H., Liu, Y., Tang, G.Q., Yang, J.H., Zhu, W.G., 2010. Precise U-Pb and Pb-Pb dating of Phanerozoic baddeleyite by SIMS with oxygen flooding technique. J. Anal. Spectr. 25, 1107–1113.

Li, X.H., Li, Z.X., Sinclair, J.A., Li, W.X., Carter, G., 2006. Revisiting the "Yanbian Terrane": implications for Neoproterozoic tectonic evolution of the western Yangtze Block, South China. Precambrian Res. 151, 14–30.

Li, X.H., Liu, Y., Li, Q.L., Guo, C.H., Chamberlain, K.R., 2009. Precise determination of Phanerozoic zircon Pb/Pb age by multi-collector SIMS without external standardization. Geochem. Geophys. Geosyst. 10, Q04010. https://doi.org/10.1029/2009GC002400.

Li, Z.X., Wartho, J.A., Occhipinti, S., Zhang, C.L., Li, X.H., Wang, J., Bao, C.M., 2007. Early history of the eastern Sibao orogen (South China) during the assembly of Rodinia: new $^{40}Ar/^{39}Ar$ dating and U-Pb SHRIMP detrital zircon provenance constraints. Precambrian Res. 159, 74–94.

Li, Z.X., Chen, H.L., Li, X.H., Zhang, F.Q., 2014. Tectonics of South China-interpreting the Rock Record. Science Press, Beijing. 144pp.

Lu, G., Wang, W., Ernst, R.E., Söderlund, U., Lan, Z., Huang, S., Xue, E., 2019. Petrogenesis of Paleo-Mesoproterozoic mafic rocks in the southwestern Yangtze Block of South China: Implications for tectonic evolution and paleogeographic reconstruction. Precambrian Res. 322, 66–84.

Meert, J.G., 2012. What's in a name? The Columbia (Paleopangaea/Columbia) supercontinent. Precambrian Res. 21, 987–993.

Meert, J.G., Santosh, M., 2017. The Columbia supercontinent revisited. Gondwana Res. 50, 67–83.

Miyashiro, A., 1974. Volcanic rock series in island arcs and active continental margins. Am. J. Sci. 274, 321–355.

Niu, Y., Regelous, M., Wendt, I.J., Batiza, R., O'Hara, M.J., 2002. Geochemistry of near-EPR seamounts: importance of source vs. process and the origin of enriched mantle component. Earth Planet. Sci. Lett. 199 (3–4), 327–345.

Pang, W.H., Ren, G.M., Sun, Z.M., Yin, F.G., 2015. Division and correlation of Paleo-Mesoproterozoic strata on the western margin of Yangtze Block: evidence from the U-Pb age of tuff zircon in the Tong'an Formation. Geol. China 42, 921–936 (in Chinese with English abstract).

Peng, M., Wu, Y.B., Gao, S., Zhang, H.F, Wang, J., Liu, X.C., Gong, H.J., Zhou, L., Hu, Z.C., Liu, Y.S., Yan, H.L., 2012. Geochemistry, zircon U-Pb age and Hf isotope compositions of Paleoproterozoic aluminous A-type granites from the Kongling terrain, Yangtze Block: constraints on petrogenesis and geologic implications. Gondwana Res. 22, 140–151.

Qi, L., Hu, J., Grégoire, D.C., 2000. Determination of trace elements in granites by inductively coupled plasma mass spectrometry. Talanta 51, 507–513.

Ribe, N.M., 1988. Dynamical geochemistry of the Hawaiian plume. Earth Planet. Sci. Lett. 88, 37–46.

Richter, F.M., McKenzie, D., 1984. Dynamical models for melt segregation from a deformable matrix. J. Geol. 92, 729–740.

Ritter, J.R.R., Jordan, M., Christensen, U.R., Achauer, U., 2001. A mantle plume below the Eifil volcanic fields, Germany. Earth Planet. Sci. Lett. 186, 7–14.

Rogers, J.J.W., Santosh, M., 2002. Configuration of Columbia, a Mesoproterozoic supercontinent. Gondwana Res. 5, 5–22.

SBG (Sichuan Bureau of Geology), 1967. Regional Geology of Huili. Unpublished geological map.

Sun, S.S., McDonough, W.F., 1989. Chemical and isotopic systematics of oceanic basalts: Implications for mantle composition and processes. In: Saunders, A.D., Norry, M.J. (Eds.), Magmatism in the Ocean Basins. Geological Society, London Special Publications vol. 42, pp. 313–345.

Sun, W.H., Zhou, M.F., Gao, J.F., Yang, Y.H., Zhao, X.F., Zhao, J.H., 2009. Detrital zircon U-Pb geochronological and Lu-Hf isotopic constraints on the Precambrian magmatic and crustal evolution of the western Yangtze block, SW China. Precambrian Res. 172, 99–126.

Wang, K., Li, Z.X., Dong, S.W., Cui, J.J., Han, B.F., Zheng, T., Xu, Y.L., 2018. Early crustal evolution of the Yangtze Craton, South China: New constraints from zircon U-Pb-Hf isotopes and geochemistry of ca. 2.9–2.6 Ga granitic rocks in the Zhongxiang complex. Precambrian Res. 314, 325–352.

Wang, L.J., Griffin, W.L., Yu, J.H., O'Reilly, S.Y., 2012. Early crustal evolution in the western Yangtze Block: evidence from U-Pb and Lu-Hf isotopes on detrital zircons from sedimentary rocks. Precambrian Res. 222–223, 368–385.

Wang, W., Zhou, M.F., 2014. Provenance and tectonic setting of the Paleo- to Mesoproterozoic Dongchuan Group in the southwestern Yangtze Block, South China: implication for the breakup of the supercontinent Columbia. Tectonophysics 610, 110–127.

Wang, W., Zhou, M.F., Zhao, X.F., Chen, W.T., Yan, D.P., 2014. Late Paleoproterozoic to Mesoproterozoic rift successions in SW China: Implication for the Yangtze Block-North Australia-Northwest Laurentia connection in the Columbia supercontinent. Sediment. Geol. 309, 33–47.

Wilson, M., 1993. Geochemical characteristics of oceanic and continental basalts: a key to mantle dynamics? J. Geol. Soc. Lond. 150, 977–990.

Wu, M.D., Duan, J.S., Song, X.L., Chen, L., Dan, Y., 1990. Geology of Kunyang Group in Yunnan Province. Scientific Press of Yunnan Province, Kunming 265 (in Chinese with English abstract).

Wyllie, P.J., 1981. Plate tectonics and magma genesis. Geol. Rundsch. 70, 128–153.

Wyllie, P.J., 1988. Magma genesis, plate tectonics and chemical differentiation of the Earth. Rev. Geophys. 26, 370–404.

Xu, Y.G., Chung, S.L., Jahn, B.M., Wu, G.Y., 2001. Petrologic and geochemical constraints on the petrogenesis of Permian-Triassic Emeishan flood basalts in southwestern China. Lithos 58, 145–168.

Xu, Y.G., He, B., Chung, S.L., Menzies, M.A., Frey, F.A., 2004. Geologic, geochemical, and geophysical consequences of plume involvement in the Emeishan flood-basalt province. Geology 32, 917–920.

Yang, B., Dong, G.C., Guo, Y., Wang, Z.Z., Wang, P., 2016. Geochemistry, zircon U-Pb geochronology and significances of the dazhupeng rhyolites in the western yangtze platform. J. Mineral. Petrol. 2, 82–91.

Zhang, C.H., Gao, L.Z., Wu, Z.J., Shi, X.Y., Yan, Q.R., Li, D.J., 2007. SHRIMP U-Pb zircon age of tuff from the Kunyang group in central Yunnan: evidence for Grenvillian orogeny in south China. Chin. Sci. Bull. 52, 1517–1525.

Zhao, G.C., Cawood, P.A., Wilde, S.A., Sun, M., 2002. Review of global 2.1–1.8 Ga orogens: Implications for a pre-Rodinia supercontinent. Earth Sci. Rev. 59, 125–162.

Zhao, X.F., Zhou, M.F., 2011. Fe–Cu deposits in the Kangdian region, SW China: a Proterozoic IOCG (iron–oxide–copper–gold) metallogenic province. Mineral. Deposita 46, 731–747.

Zhao, X.F., Zhou, M.F., Li, J.W., Sun, M., Gao, J.F., Sun, W.H., Yang, J.H., 2010. Late Paleoproterozoic to early Mesoproterozoic Dongchuan Group in Yunnan, SW China: implications for tectonic evolution of the Yangtze Block. Precambrian Res. 182, 57–69.

Zhou, M.F., Zhao, X.F., Chen, W.T., Li, X.C., Wang, W., Yan, D.P., Qiu, H.N., 2014. Proterozoic Fe-Cu metallogeny and supercontinental cycles of the southwestern Yangtze Block, southern China and northern Vietnam. Earth Sci. Rev. 139, 59–82.

Zhu, L.G., Liu, J.J., Bagas, L., Carranza, E.J.M., Zhai, D.G., Meng, G.Z., Wang, J.P., Wang, Y.H., Zhang, F.F., Liu, Z.J., 2019. The Yinachang Fe-Cu-Au-U-REE deposit and its relationship with intermediate to mafic intrusions, SW China: Implications for ore genesis and geodynamic setting. Ore Geol. Rev. 104, 190–207.

Zhu, W.G., Bai, Z.J., Zhong, H., Ye, X.T., Fan, H.P., 2016a. The origin of the c. 1.7 Ga gabbroic intrusion in the Hekou area, SW China: constraints from SIMS U-Pb zircon geochronology and elemental and Nd isotopic geochemistry. Geol. Mag. 154, 286–304.

Zhu, W.G., Zhu, W.G., Li, Z.X., Bai, Z.J., Yang, Y.J., 2016b. SIMS zircon U-Pb ages, geochemistry and Nd–Hf isotopes of ca. 1.0 Ga mafic dykes and volcanic rocks in the Huili area, SW China: Origin and tectonic significance. Precambrian Res. 273, 67–89.

Zhu, Z.M., Tan, H.Q., Liu, Y.D., 2017. Late Palaeoproterozoic Hekou Group in Sichuan, Southwest China: geochronological framework and tectonic implications. Int. Geol. Rev. 60, 305–318.